Journal of Power Sources 195 (2010) 2956–2960

Contents lists available at ScienceDirect

Journal of Power Sources

journal homepage: www.elsevier.com/locate/jpowsour

Short communication

Interfacial properties between $LiFePO_4$ and poly(ethylene oxide)–$Li(CF_3SO_2)_2N$ polymer electrolyte

K. Hanai*, K. Kusagawa, M. Ueno, T. Kobayashi, N. Imanishi, A. Hirano, Y. Takeda, O. Yamamoto

Department of Chemistry, Faculty of Engineering, Mie University, 1577 Kurimamachiyacho, Tsu, Mie 514-8507, Japan

ARTICLE INFO

Article history:
Received 2 June 2009
Received in revised form 31 August 2009
Accepted 31 August 2009
Available online 6 September 2009

Keywords:
Polymer electrolyte
Poly(ethylene oxide) (PEO)
$LiFePO_4$
Charge transfer resistance

ABSTRACT

The interface resistance between Li_xFePO_4 and poly(ethylene oxide) (PEO)–$Li(CF_3SO_2)_2N$ (LiTFSI) was examined by AC impedance measurement of a Li_xFePO_4/PEO–LiTFSI/Li_xFePO_4 cell in the temperature range of 30–60 °C. Four types of resistance, R0, R1, R2 and R3 were proposed according to analysis of the cell impedance using an equivalent circuit. The sum of R0 and R1 in the high frequency range is consistent with the resistance of the PEO electrolyte. R2 in the middle frequency range is related to lithium ion transport to an active point for charge transfer inside the composite electrode, and R3 in the low frequency range is considered to be the charge transfer resistance. The activation energy for R2 was affected by the thickness and composition of the electrode, whereas that for R3 was not.

1. Introduction

Rechargeable solid lithium polymer batteries (SLPBs) are considered to be a promising candidate for large-scale batteries in electric vehicles (EV), plug-in hybrid vehicles (PHEV), and as back-up storage for solar cells, because of their low production cost, high reliability, safety, and flexibility for cell design [1,2]. Conventional SLPBs have used lithium metal anodes and oxide cathodes such as V_2O_5 to ensure high-energy density [3]. However, this type of SLPB, with a lithium metal anode, has been reported to have serious safety problems. Recently, Imanishi et al. reported the possibility of using a carbon anode with a solid lithium polymer electrolyte [4]. A carbon anode could be coupled with cathode materials containing lithium, such as $LiCoO_2$, $LiMn_2O_4$, and $LiFePO_4$. However, the choice of cathode materials is somewhat restricted by the thermodynamic stability of the polymer electrolyte. The stability window of typical solid polymer electrolytes, such as poly(ethylene oxide) (PEO) based electrolytes, does not exceed 4 V vs. Li/Li^+ [5]. The typical cathode materials for lithium ion batteries, such as $LiCoO_2$ and $LiMn_2O_4$, cannot be used for the cathode in PEO electrolyte cells, because their working potentials are around 4 V vs. Li/Li^+. Croce et al. reported that $LiFePO_4$ was the best candidate for the cathode material in SLPBs with PEO based electrolyte, due to the low volume change by lithium insertion and extraction, a low working potential of 3.5 V vs. Li/Li^+, low cost, and a high thermal decomposition temperature [6]. A reversible capacity of 140 mAh g^{-1} at 100 °C was observed for a Li/PEO–$LiCF_3SO_3$/$LiFePO_4$ cell, which is comparable with 165 mAh g^{-1} obtained for Li/PC-DMC–$LiPF_6$/$LiFePO_4$ at room temperature [7]. In previously reported solid lithium polymer cells with $LiFePO_4$ cathodes, high capacity was observed only at higher temperatures and low current density, such as 0.05 mA cm^{-2} [8]. The charge–discharge performance of SLPBs is strongly dependent on the interface resistance between the electrode and the electrolyte, especially at low temperature [9,10].

In our previous work, we reported the low temperature performance of a Li/PEO–LiTFSI/$LiFePO_4$ cell; the interfacial resistance between PEO–LiTFSI and $LiFePO_4$ was not significantly dependent on the molecular weight of PEO and the content of LiTFSI in PEO [11,12]. In this study, the interface resistance between Li_xFePO_4 and PEO–LiTFSI was examined using a symmetrical Li_xFePO_4/PEO–LiTFSI/Li_xFePO_4 cell and the interface resistances were analyzed as a function of the operation temperature and the electrode composition (x in Li_xFePO_4).

2. Experimental

The PEO based electrolyte was prepared according to the previously reported solvent casting technique with acetonitrile (AN) as a solvent [13]. PEO (Aldrich Chemical, average molecular weight 6×10^5) and $Li(CF_3SO_2)_2N$ (LiTFSI, Wako) were dissolved in AN with a molar ratio of Li/O = 1/10. The polymer electrolyte solution was cast in a polytetrafluoroethylene (PTFE) dish under a dry argon atmosphere. After evaporation of AN at room temperature, the film was dried at 110 °C for 12 h under vacuum. The thicknesses of the

* Corresponding author. Tel.: +81 59 231 9420; fax: +81 59 231 9478.
E-mail address: hanai@m.mie-u.ac.jp (K. Hanai).

0378-7753/$ – see front matter © 2009 Elsevier B.V. All rights reserved.
doi:10.1016/j.jpowsour.2009.08.087

polymer electrolytes used for AC impedance measurements and charge–discharge tests were ca. 500 μm, and ca. 1 mm for conductivity measurements.

The cathode electrodes consisted of carbon-coated $LiFePO_4$ (Hohsen Co., carbon content 2.0 wt%, average particle size 3.3 μm), vapor grown carbon fiber (VGCF; Showa Denko, Japan, average diameter 150 nm, length ca. 20 μm) and the polymer electrolyte mixed in AN (4:1:5 weight ratio). The solution was painted on aluminum foil and the AN solvent was allowed to slowly evaporate at room temperature under a dry argon atmosphere, and was then dried at 110 °C for 12 h under vacuum. The electrode film thickness was in a range of 20–70 μm and the active electrode area was 2.25 cm^2 (1.5 cm × 1.5 cm). The reversible capacity of the composite $LiFePO_4$ electrode at 50 °C was 140 mAh g^{-1} at 1/10 °C and 100 mAh g^{-1} at 3 °C.

A target for sputtering $LiFePO_4$ was prepared by a solid state reaction method [14]. Li_2CO_3, $FeC_2O_4{\cdot}H_2O$ and $(NH_4)H_2PO_4$ powders (Nacalai Tesque) were mixed in a 1:2:2 molar ratio. The mixture was ground and pressed into a tablet, which was then sintered at 700 °C for 6 h under 2% H_2–Ar. The product was crushed and the procedure repeated. The final powder was pressed into a tablet of 5.5 cm in diameter as the sputtering target. The $LiFePO_4$ film was deposited on Au foil by RF magnetron sputtering (Ulvac, SCOTT-C3). Sputtering of $LiFePO_4$ was carried out for 15 min in pure Ar at a working pressure of 2×10^{-2} Torr. The as-sputtered $LiFePO_4$ film was then annealed at 700 °C under 2% H_2–Ar. The thickness of the electrode was approximately 500 nm, as measured by cross sectional observation of scanning electron microscope image (SEM; Hitachi, S-2300S).

The conductivities of the polymer electrolytes were measured using a symmetrical blocking cell, Cu/PEO–LiTFSI/Cu. A symmetrical non-blocking cell was used to measure the interfacial resistance between the electrolyte and the electrode. The lithium content in Li_xFePO_4 was changed using an Al/Li_xFePO_4/PEO–LiTFSI/SS-mesh/PEO–LiTFSI/Li_xFePO_4/Al cell (SS: stainless steel). The cell was assembled with two working electrodes arranged face to face. A constant current was passed between the SS-mesh and the Al foil as a current corrector to deposit Li metal on the SS-mesh. AC impedance measurements of the electrolyte were performed in the temperature range of 30–60 °C. An AC perturbation of 10 mV was applied in the frequency range from 1×10^6 to 0.1 Hz using a Solartron1260 frequency response analyzer. In order to ensure good contact between the electrolyte and electrode, the cells were initially heated to 80 °C and then cooled down to the measurement temperature.

3. Results and discussion

Fig. 1 shows the impedance spectrum of a symmetrical cell (Al/$Li_{0.98}FePO_4$-C/PEO_{10}LiTFSI/$Li_{0.98}FePO_4$-C/Al) at 50 °C, in which there are four major resistance components. These resistance components are a simple ohmic resistance (R0), a resistance in the high frequency range (small semicircle, R1), a resistance in the middle frequency range (semicircle, R2), and a resistance in the low frequency range (large semicircle, R3). The R0 and R1 resistances have the same profiles as that observed for Cu/PEO_{10}LiTFSI/Cu. Therefore, both R0 and R1 are assigned to the resistances of the PEO electrolyte which are caused by the ionic transport through mixed phases of crystalline and amorphous domains occurred at room temperature. Fig. 2 shows the impedance profiles of a symmetrical cell (Al/Li_xFePO_4-C/PEO_{10}LiTFSI/Li_xFePO_4-C/Al) at 50 °C as a function of x in Li_xFePO_4. The Li content in Li_xFePO_4 was changed *in situ* using a third SS-mesh electrode inserted into the polymer electrolyte, as described in Section 2. The electrode containing $LiFePO_4$ exhibits blocking behavior with a vertical spike,

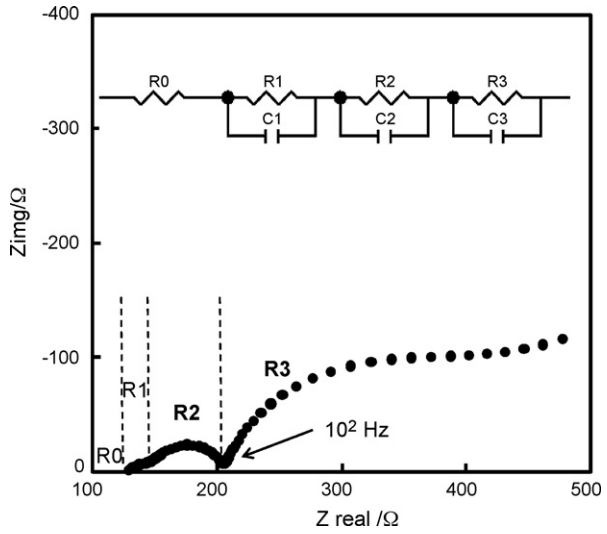

Fig. 1. Impedance spectrum for Al/$Li_{0.98}FePO_4$/PEO_{10}LiTFSI/$Li_{0.98}FePO_4$/Al at 50 °C.

and only two semicircles are observed. Saturation of the $LiFePO_4$ structure with lithium ions is indicated by the blocking characteristics, whereas lithium deficient $Li_{0.98}FePO_4$ exhibits non-blocking behavior. The R2 and R3 resistance values were obtained by fitting the experimental data using the equivalent circuit shown in Fig. 1. The compositional dependence of R2 and R3 is shown in Fig. 3. R2 (10^4–10^3 Hz) increases and R3 (10–1 Hz) decreases with decreasing x in Li_xFePO_4. R3 changed reversibly and R2 irreversibly with the change in x, which suggests that R3 corresponds to the charge transfer resistance between the polymer electrolyte and Li_xFePO_4. Srinivasan and Newman [15] reported that Li_xFePO_4 was a two phase mixture of $LiFePO_4$ and $FePO_4$ in the range $x = 0.9525$–0.002. Therefore, the active area for the charge transfer reaction increases with decreasing x, which results in a decrease of the charge transfer resistance. Bruce [16] and Franger et al. [17] reported similar impedance profiles for cells with a polymer electrolyte and liquid electrolyte, respectively. They suggested that the two semicircles are consistent with a complex electrochemical reaction that involves more than a simple electron transfer between the redox couple and the electrode. The reaction may

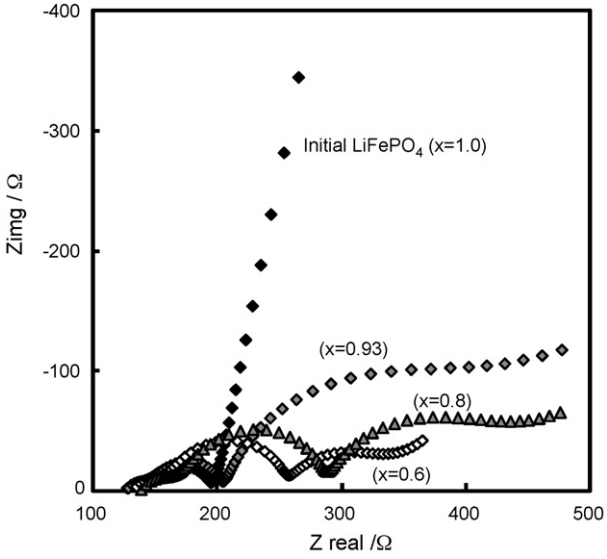

Fig. 2. Impedance spectra for Al/Li_xFePO_4/PEO_{10}LiTFSI/Li_xFePO_4/Al at 50 °C for various x in Li_xFePO_4.

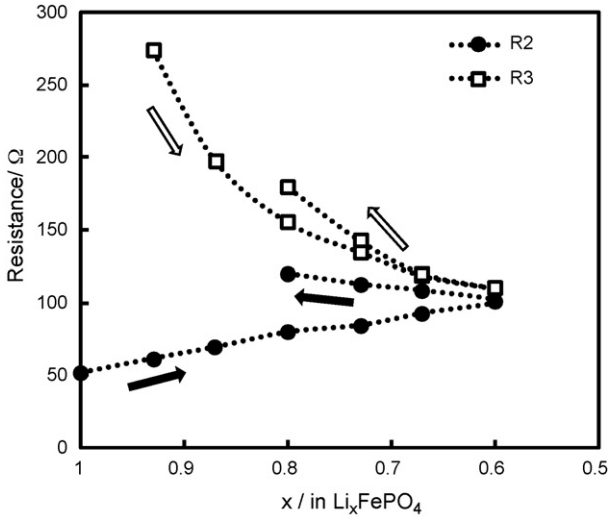

Fig. 3. Interface resistances of R2 and R3 as a function of x in Li_xFePO_4 at 50 °C.

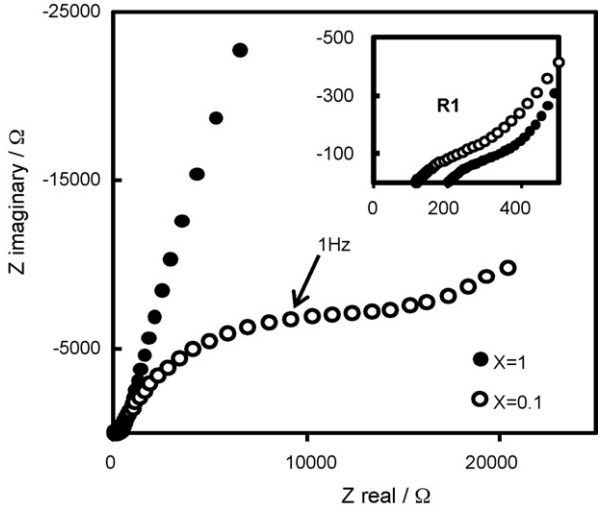

Fig. 5. Impedance spectra for Au/sputtered Li_xFePO_4/PEO_{10}LiTFSI/sputtered Li_xFePO_4/Au at 50 °C.

involve adsorption or a chemical step in addition to the charge transfer process. The impedance spectra of $LiFePO_4$ with a liquid electrolyte, as reported by Shin et al. [18], showed two depressed semicircles, and those by Takahashi et al. [19] only one depressed semicircle; however, these reports did not report the content of Li in Li_xFePO_4.

To clarify the origin of R2 and R3, the cell impedance of Al/$Li_{0.98}FePO_4$-C/PEO_xLiTFSI (x = 10 and 18)/$Li_{0.98}FePO_4$-C/Al was measured and the temperature dependence of R2 and R3 are shown in Fig. 4. PEO–LiTFSI has a knee in the conductivity curve at around 60 °C, which corresponds to the phase transition temperature of the electrolyte. PEO_{18}LiTFSI has a conductivity knee at near 50 °C, and PEO_{10}LiTFSI shows no clear phase transition behavior until 30 °C [20,21]. R2 and R3 for the cell with PEO_{10}LiTFSI exhibits no clear knee in the temperature range measured. In contrast, R2 observed in the cell with PEO_{18}LiTFSI has a jump in conductivity near 50 °C and R3 is a straight line. The activation energies of R3 for PEO_{10}LiTFSI and PEO_{18}LiTFSI were calculated as 75 and 87 kJ mol^{-1}, respectively. The activation process for R3 is not affected by the electrolyte phase transition, which suggests that R3 could be considered as the charge transfer resistance. On the other hand, the R2 resistance is affected by the phase transition of the polymer electrolyte; R2 with PEO_{18}LiTFSI jumps at around 50 °C, the temperature that corresponds to the phase transition of the polymer electrolyte. Therefore, R2 could be attributed to an ion transfer to the active site for charge transfer in the composite electrode.

To confirm the effect of the additive in the electrode, a $LiFePO_4$ thin film electrode was prepared by RF sputtering on an Au substrate to eliminate the effect of the polymer electrolyte and the conductive VGCF additive in the composite electrode. The obtained sputtered film had the same XRD pattern as that for powdered $LiFePO_4$. The thickness of the film estimated from SEM images was approximately 500 nm. Fig. 5 shows impedance spectra of a symmetrical cell with the sputtered $LiFePO_4$ thin film electrode and PEO_{18}LiTFSI electrolyte at 50 °C. The as-sputtered electrode exhibits blocking behavior and only the sum of PEO_{18}LiTFSI resistance, R0–R1, is obtained, that is, the composition of the film is considered to be $LiFePO_4$. Lithium was extracted from $LiFePO_4$ using the SS-mesh in the polymer electrolyte. The impedance profile of $Li_{0.1}FePO_4$ is also shown in Fig. 5. A small semicircle in the high frequency range and a large depressed semicircle are observed. The first semicircle corresponds to the resistance of the polymer electrolyte. The frequency range of the second semicircle is similar that of R3 for the composite electrode shown in Fig. 2. It should be emphasized that the thin film electrode without the polymer electrolyte and the conductive VGCF additive has no semicircle in the intermediate frequency range, which corresponds to R2. Therefore, R2 can be reasonably assigned from its arising frequencies to

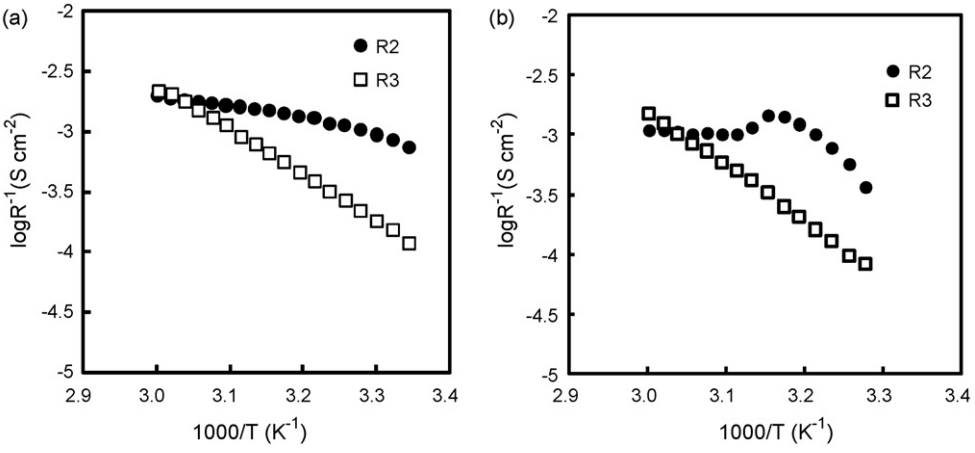

Fig. 4. Temperature dependence of the interface resistance of R2 and R3 measured for cells with different polymer electrolytes. (a) Al/$Li_{0.98}FePO_4$/PEO_{10}LiTFSI/$Li_{0.98}FePO_4$/Al and (b) Al/$Li_{0.98}FePO_4$/PEO_{18}LiTFSI/$Li_{0.98}FePO_4$/Al.

Table 1
Dependence of the interface resistance and activation energy on electrode thickness of the $LiFePO_4$:VGCF:$(PEO)_{10}$LiTFSI (4:1:5 weight ratio) composite electrode in the temperature range of 60–40 °C.

Electrode properties		Resistance at 50 °C (x = 0.7)			Activation energy	
Thickness, μm	Weight, mg cm^{-2}	Active material weight, mg cm^{-2}	R2, Ω cm^{-2}	R3, Ω cm^{-2}	R2, kJ mol^{-1}	R3, kJ mol^{-1}
21	1.1	0.4	616	1796	6	63
36	3.6	1.4	167	580	26	73
56	6.0	2.4	149	225	40	70

Table 2
Dependence of the interface resistance and activation energy on the electrode composition of the $LiFePO_4$-VGCF–PEO_{10}LiTFSI composite electrode.

Electrode composition	Electrode properties			Resistance at 50 °C (x = 0.7)		Activation energy	
($LiFePO_4$-VGCF):(PEO_{10}LiTFSI)	Thickness, μm	Weight, mg cm^{-2}	Active material weight, mg cm^{-2}	R2, Ω cm^{-2}	R3, Ω cm^{-2}	R2, kJ mol^{-1}	R3, kJ mol^{-1}
40:60	42	3.1	0.97	653	527	10	67
70:30	44	4.4	1.0	180	324	44	76

the ionic transport in the polymer electrolyte inside the composite electrode. The linear increase in the resistance may be attributed to the SEI formation near the boundary between polymer and $LiFePO_4$ particles. An Arrhenius plot of the R3 resistance for the sputtered electrode with PEO_{18}LiTFSI is shown in Fig. 6. The activation energy calculated from the temperature dependence is 77 kJ mol^{-1}, the value of which is comparable to that of the composite electrode with PEO_{18}LiTFSI, as shown in Fig. 4. It is concluded that R2 is dominated by the polymer electrolyte in the composite electrode, and R3 is due to the charge transfer resistance between the polymer electrolyte and Li_xFePO_4.

The influence of electrode thickness on the interface resistance of the composite electrode with $LiFePO_4$-C:VGCF:PEO_{10}LiTFSI (4:1:5 weight ratio) was examined in the temperature range of 60–40 °C and the results are summarized in Table 1. R2 and R3 decrease with increasing electrode thickness. These resistances depend on the surface area of Li_xFePO_4-C/polymer electrolyte, which are enlarged by increasing the thickness of the electrode. This clearly indicates that R2 is assigned to the ionic transport across the polymer layer formed on the $LiFePO_4$ particles. Activation energies for R3 revealed no significant change with the thickness. On the other hand, the activation energies for R2 show a clear dependence on the thickness, and that of a thick 56 μm electrode was

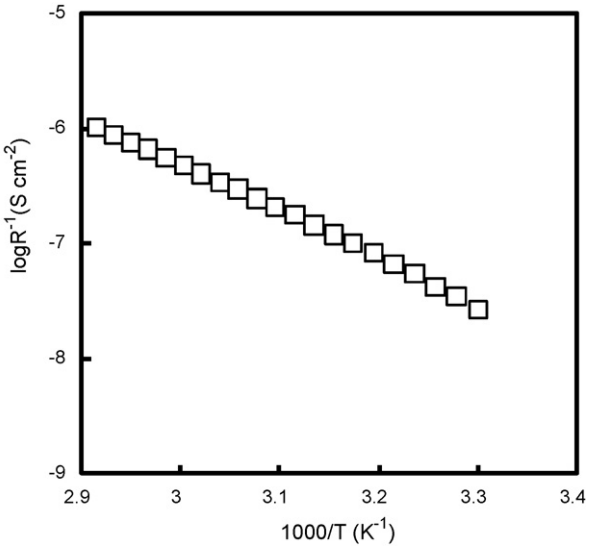

Fig. 6. Arrhenius plot of the R3 interface resistance obtained for Au/sputtered Li_xFePO_4/PEO_{10}LiTFSI/sputtered Li_xFePO_4/Au.

40 kJ mol^{-1}. The value of the activation energy is comparable to that for the electrical conductivity of PEO_{10}LiTFSI, which suggests that the diffusion of lithium ions in the polymer electrolyte with a thick composite electrode is the rate determining step for R2. Table 2 shows the dependence of the ratio of electrode materials ($LiFePO_4$-C, VGCF) and PEO_{10}LiTFSI on R2 and R3. R2 and R3 decrease with decreasing polymer electrolyte content in the electrode. Activation energies for R3 have no dependence on the polymer electrolyte content of the electrode. In contrast, the activation energy for R2 increases with decreasing polymer electrolyte content in the electrode. The frequency range of R2 is slightly lower than that of the bulk polymer electrolyte. It is considered that the R2 resistance is dominated by the PEO electrolyte within the electrode; the segmental conduction polymer is restricted to of lithium ions due to the complicated structure of the electrode.

4. Conclusions

The interface resistance between Li_xFePO_4 and PEO–LiTFSI was examined using AC impedance measurements with a symmetrical cell in the temperature range of 30–60 °C. Four resistances, R0, R1, R2 and R3 were distinguished. The resistances in the high frequency region (R0 and R1) were considered to be resistance of the PEO electrolyte. R2 and R3 are dependent on x in Li_xFePO_4 and this dependence suggests that R3 in the low frequency region is related to the charge transfer resistance. R2 was considered to be related to the internal resistance of the composite electrode, because the sputtered $LiFePO_4$ electrode had no semicircle corresponding to R2 in the same frequency range. The activation energy for R2 was affected by the thickness and composition of the electrode. The activation energy for a thick composite electrode with a low content of polymer electrolyte was comparable to that of the polymer electrolyte. On the other hand, the activation energy for R3 was not affected by the thickness and composition of the electrode.

Acknowledgements

This study was supported by the Cooperation of Innovative Technology and Advanced Research in Evolution Area (City Area) Project from the Ministry of Education, Sports, Science and Technology of Japan.

References

[1] B. Scrosati, F. Croce, S. Panero, J. Power Sources 100 (2001) 93–100.
[2] M. Gauthier, D. Fauteux, G. Vassort, A. Bélanger, M. Duval, P. Ricoux, J.-M. Chabagno, D. Muller, P. Rigaud, M.B. Armand, D. Deroo, J. Electrochem. Soc. 132 (1985) 1333–1340.

[3] G.B. Appetecchi, J.H. Shin, F. Alessandrini, S. Passerini, J. Power Sources 143 (2005) 236–242.
[4] N. Imanishi, Y. Ono, K. Hanai, R. Uchiyama, Y. Liu, A. Hirano, Y. Takeda, O. Yamamoto, J. Power Sources 178 (2008) 744–750.
[5] Y. Xia, K. Tatsumi, T. Fujieda, P.P. Prosini, T. Sakai, J. Electrochem. Soc. 147 (2000) 2050–2056.
[6] F. Croce, F.S. Fiory, L. Persi, B. Scrosati, Electrochem. Solid-State Lett. 4 (2001) A121–A123.
[7] A. Yamada, S.C. Chung, K. Hinokuma, J. Electrochem. Soc. 148 (2001) A224–A229.
[8] G.B. Appetecchi, J. Hassoun, B. Scrosati, F. Croce, F. Cassel, M. Salomon, J. Power Sources 124 (2003) 246–253.
[9] Q. Li, T. Itoh, N. Imanishi, A. Hirano, Y. Takeda, O. Yamamoto, Solid State Ionics 159 (2003) 97–109.
[10] Q. Li, N. Imanishi, Y. Takeda, A. Hirano, O. Yamamoto, Electrochem. Solid-State Lett. 7 (2004) A470–A473.
[11] K. Hanai, T. Matsumura, N. Imanishi, A. Hirano, Y. Takeda, O. Yamamoto, J. Power Sources 178 (2008) 789–794.
[12] K. Hanai, R. Uchiyama, N. Imanishi, A. Hirano, Y. Takeda, O. Yamamoto, J. Jpn. Soc. Power Powder Metall. 56 (2009) 71–75.
[13] C. Capiglia, J. Yang, N. Imanishi, A. Hirano, Y. Takeda, O. Yamamoto, J. Power Sources 119–121 (2003) 826–832.
[14] K.F. Chiu, H.Y. Tang, B.S. Lin, J. Electrochem. Soc. 154 (2007) A364–A368.
[15] V. Srinivasan, J. Newman, J. Electrochem. Soc. 151 (2004) A1517–A1529.
[16] P.G. Bruce, Electrochim. Acta 40 (1995) 2077–2085.
[17] S. Franger, S. Bach, J. Farcy, J.-P. Pereira-Ramos, N. Baffier, Electrochim. Acta 48 (2003) 891–900.
[18] H.C. Shin, W.H. Cho, H. Jang, Electrochim. Acta 52 (2006) 1472.
[19] M. Takahashi, S. Tobishima, K. Takei, Y. Sakurai, Solid State Ionics 148 (2002) 283–289.
[20] S. Lascaud, M. Perrier, A. Vallée, S. Besner, J. Prud'homme, M. Armand, Macromolecules 27 (1994) 7469–7477.
[21] C. Labrèche, I. Lévesque, J. Prud'homme, Macromolecules 29 (1996) 7795–7801.